Proceedings World Geothermal Congress 2000
Kyushu - Tohoku, Japan, May 28 - June 10, 2000

LONG-TERM PERFORMANCE OF HEAT MINIG IN HOT AQUIFERS: WATER-ROCK INTERACTION AND PERMEABILITY CHANGES

Hansgeorg Pape[1], Jörn Bartels[2], Michael Kühn[3], and Christoph Clauser[4]
[1]Geodynamik, Rheinische Friedrich-Wilhelms-Universität, Nussallee 8, D-53115 Bonn, Germany
[2]Landesamt für Umwelt, Naturschutz und Geologie (LUNG) Mecklenburg-Vorpommern, Geologischer Dienst, PF 160143, D-19061 Schwerin, Germany
[3]Wasserwirtschaft und Wasserversorgung, TU Hamburg-Harburg, Schwarzenbergstr. 95, D-21073 Hamburg, Germany
[4]Geowissenschaftliche Gemeinschaftsaufgaben (GGA), PF 510153, D-30631 Hannover, Germany

Key Words: geothermal, geochemical, permeability, reservoir evaluation

ABSTRACT

We simulate the effect of chemical induced changes in the pore space structure of porous aquifers on flow and transport using a new numerical code developed in an interdisciplinary project of 3-year duration. The three key elements of this new simulation approach are: (1) a relationship between changes in porosity and permeability which is based on petrophysical principles; (2) a chemical model for precipitation and dissolution reactions at high temperature and salinity; (3) a numerical simulation tool for coupled flow, heat and multi-component transport, and chemical water-rock interaction. The derivation of the new relationship between porosity and permeability comprises the application of a fractal model of the pore space structure and its change due to precipitation and dissolution of minerals. Permeability is expressed as a power series of porosity. Based on the Kozeny-Carman equation (Carman, 1956) the exponents of this series are calculated from the fractal dimension of the fluid-rock interface which is a fundamental structural parameter in our approach. This expression was calibrated and validated with large petrophysical data sets from clean and shaly sandstones. This way, a set of curves was obtained in a permeability-porosity plot in which each curve is characteristic for one type of sandstone. The geochemical reaction model is based on the speciation code PHRQPITZ (Plummer et al., 1988). Following our code extension and update of its thermo-dynamic data base it is now valid for brines of low to high (5 mol/l) ionic strength and temperatures of 0–150 °C. Reaction kinetics was added to account for the fact that under- or over-saturation does not always trigger dissolution or precipitation, which was observed in the laboratory as well as in geothermal installations under operation. With this new numerical tool coupled, three-dimensional simulations can be run for total operation times of 30-100 years and different production/injection regimes, types of fluid mineralization, and fractal dimensions of the precipitating mineral surface. It turns out that most changes in the system occur at the propagating temperature front and in the vicinity of the injection well due to the complex interaction of all coupled processes. Finally, we identify critical scenarios for the operation of a hydrothermal heat mining installation over a period of 30–50 years.

1. INTRODUCTION

A hydrothermal heat mining installation is a major investment. In order to pay off, operation times of 30 years and more are required during which a sufficient amount of hot water can be produced. In this context, numerical simulations of flow, heat and species transport, and water-rock interaction are helpful to predict a reservoir's long-term performance under operation. Of particular interest are changes of the hydraulic properties of the reservoir rock brought about by technical operations at the production or injection wells, which offset the chemical equilibrium between minerals of the reservoir rock and reservoir fluid. This, in turn, causes transport of chemical species, solution and precipitation of minerals in the pore space of the rock as a function of space and time. These heterogeneous chemical reactions change the pore space structure and alter its porosity and permeability. Therefore our simulation approach comprises coupled flow and heat transport, multi-component species transport, a geochemical reaction model, and a petrophysical model providing a relation for changes in permeability caused by changes in porosity. In this paper we focus on this particular relationship between porosity and permeability in sandstones in general and on permeability changes induced by precipitation of minerals. In addition, Pape et al. (1999) showed how this theory can be applied to derive permeability logs from standard geophysical borehole logs.

2. PERMEABILITY-POROSITY RELATIONSHIP

Changes in porosity ϕ can be calculated without difficulty from the reaction rates of the mineral components. However, it is not as straightforward to estimate the associated changes in permeability k, because permeability depends not only on the bulk porosity but also strongly on the structure of the pore space. Therefore it is not possible to present one single equation which relates permeability to porosity for all rock types. In the past, different empirical approaches were used to describe the observed highly nonlinear dependence of permeability on porosity by exponential or power-law relationships. However, these purely empirical approaches lack a petrophysical motivation. For porosities larger than 10 % the slopes of different linear regressions in the $\log(k)$ versus $\log(\phi)$ plot vary from 3 to 10.

Petrophysical model theory provides different permeability-porosity relationships. Relatively simple models consisting of a bundle of smooth capillaries or of a packing of smooth spheres are successful to describe the behavior of clean sandstones with high porosity. These models lead to a

frequently used equation which has porosity taken to the third power (e.g. Ungerer, 1990):

$$k = 0.5\ (r_{grain})^2\ \phi^3 / (1-\phi)^2\ , \qquad (1)$$

where r_{grain} is the radius of model grains.

The compaction of sedimentary rocks during diagenesis was described by overlapping spheres (van der Marck, 1999) or by network models (David *et al*.,1994; Zhu *et al*., 1995). These theoretical approaches are useful to predict changes in permeability and porosity due to mechanical compaction and pressure dissolution, preferably for clean sandstones, such as the Fontainebleau sandstone. For this material Bourbie and Zinszner (1985) found a good fit between permeability and porosity for the following relation:

$$k = 303\ (100\phi)^{3.05} \quad (\mathrm{nm}^2) \text{ for } \phi > 0.08, \qquad (2a)$$

$$k = 0.0275\ (100\phi)^{7.33}\ (\mathrm{nm}^2) \text{ for } \phi \le 0.08. \qquad (2b)$$

However, the Fontainebleau sandstone does not represent the average type of sandstone which is characterized by a large pore size distribution and highly structured pore walls. A model which is particularly close to the natural appearance of pore space in sedimentary rocks is the so-called "pigeon hole“ model, of Pape *et al*. (1982, 1984, 1987 a,b). It is based on data from core samples of various hydrocarbon reservoir rocks in northwest Germany. It yields petrophysically justified relations between various geometric, storage, and transport parameters of these reservoir rocks. Like other fractal models, it is based on the observation that the shape of the internal surface of rock pores follows a self-similar rule. Thus, the theory of fractals can be applied. A key parameter in this theory is the fractal dimension *D*.

This model is combined with the Kozeny-Carman equation (Carman, 1956) which links permeability to the effective pore radius and the formation factor *F*. This yields a general permeability-porosity relationship:

$$k = \mathrm{A}\ \phi + \mathrm{B}\ \phi^{\exp 1} + \mathrm{C}\ (10\phi)^{\exp 2} \qquad (3)$$

where the exponents exp1 and exp2 depend on the fractal dimension and the coefficients need to be calibrated for each sedimentary basin.

2.1 Theory

A fundamental expression for the permeability *k* of a porous medium is given by the modified Kozeny-Carman equation:

$$k = r^2_{eff} / (8F)\ , \qquad (4)$$

where *F* is the formation factor, which is defined as the ratio of tortuosity *T* and porosity ϕ:

$$F = T / \phi\ . \qquad (5)$$

The formation (resistivity) factor is originally defined as the ratio of the resistivity of a porous medium saturated with an electrolyte and the resistivity of this electrolyte. It is a purely geometric parameter, which describes the way in which the porous medium obstructs transport processes, such as the passage of ions or even uncharged molecules. It is related to permeability via the Kozeny-Carman equation (4). Pape et al. (1987a) showed that tortuosity behaves as a fractal and depends on the ratio of effective hydraulic radius r_{eff} and grain radius r_{grain}, (see Figure 1) taken to a power which is a function of the fractal dimension *D*:

$$T = 1.34\ (\ r_{grain} / r_{eff}\ )^{0.67\,(D-2)}. \qquad (6)$$

This implies that tortuosity increases with increasing fractal dimension. However, this relation is valid only in the range of $2<D<2.4$. An empirical relationship between *F* and ϕ is expressed by Archie's first law:

$$F = a/\phi^{\,m}\ . \qquad (7)$$

Here *a* is a factor which depends on lithology, and *m* is the cementation or tortuosity factor which depends on rock structure. The parameters *a* and *m* vary in the ranges $0.6 < a < 2$, and $1 < m < 3$. Archie's law (equation 4) was later also formally derived, starting from a fractal model for porous rocks by Pape and Schopper (1988) and Shashwati and Tarafdar (1997). For instance, for a pigeon hole model of common sandstones (Figure 1) this derivation starts from equation (5), which expresses *F* by tortuosity *T* and porosity ϕ, and the following equations (Pape et al., 1987) which express the fractal relationship between *T* and ϕ:

$$T = 1.34\ (r_{grain}/r_{eff})^{0.67\,(D-2)} = 1.34\ (r_{grain} / r_{eff})^{0.24}, \qquad (8)$$

$$\phi = 0.534\ (r_{grain}/r_{eff})^{0.39\,(D-3)} = 0.5\ \ (r_{grain} / r_{eff})^{-0.25}\ , \qquad (9)$$

with D=2.36. Neglecting slight differences in the exponents, equations (8) and (9) for tortuosity and porosity yield

$$T \approx 0.67 / \phi \qquad (10)$$

and

$$r^2_{eff} = r^2_{grain}\ (2\phi)^8\ . \qquad (11)$$

Using the Kozeny-Carman equation (4), the formation factor, equation (5), tortuosity, equation (10), the effective radius, equation (11) with the default value r_{grain} = 200 000 nm (an average grain radius in our sandstone data sets), *k* can now be written as

$$k = 191\ (10\ \phi)^{10} \quad (\text{in nm}^2). \qquad (12)$$

Equation 12 for permeability defines a linear asymptote in a log-log plot of *k* versus ϕ. It is valid for porosities greater than 0.1, whereas for lower porosities the measured permeabilities exceed those predicted by equation (12). An explanation is indicated by the effective pore radii of the investigated samples, which do not decrease as rapidly with decreasing porosity as suggested by equation (11) for the effective radius. For the medium range of porosities $0.01<\phi<0.1$ we can improve the permeability estimates by assigning a fixed value to the effective hydraulic pore radius in the Kozeny-Carman equation, equation (4): $r_{eff}=r_{eff,\,fix}$=200 nm. This is equal or near the mean of values for the effective hydraulic pore radius determined for medium range porosities from equations (4), (5), and (10) from measured permeabilities and porosities. Instead of equation (12) for permeability, a combination of the

Kozeny-Carman equation (4), the formation factor, equation (5), and tortuosity, equation (10), yields:

$$k = \phi^2 r^2_{eff,fix} / (8(0.67) = 7463\phi^2 \ (\text{in nm}^2). \qquad (13)$$

For very low porosities < 0.01 this expression still yields permeabilities that are too small compared to the data. The values for the effective hydraulic pore radius determined for this porosity range from measured permeabilities and porosities and equations (4), (5), and (10) are clearly smaller than 200 nm, but not smaller than 50 nm. For this range it therefore makes sense to assume a fixed minimum value $r_{eff,\,min}$ = 50 nm and a fixed maximum tortuosity T_{max} = 10 (Pape et al., 1987b). According to equation (10) for tortuosity, equation (13) for permeability then reads

$$k = \phi\, r^2_{eff,\,min} / 8\, T_{\max} = 31\phi \ (\text{in nm}^2). \qquad (14)$$

The sum of the expressions for permeability in equations (12), (13), and (14) provides an approximation of the permeability for the entire range of porosity:

$$k = 31\phi + 7463\phi^2 + 191(10\phi)^{10} \quad (\text{in nm}^2). \qquad (15)$$

The linear combination of the expressions for the low, medium, and high porosity ranges is permissible since for a given porosity, the expressions for the other two porosity ranges do not contribute significantly, due to the difference in the powers of porosity. The third term in the average permeability-porosity relationship, equation (15), characterizes the fractal behavior of sandstones, and the power of 10 reflects the fractal dimension D=2.36. Deviations from this value of the fractal dimension result in powers other than -0.25 in equation (9) for porosity. This results in a correspondingly modified exponent for the third term in the average permeability-porosity relationship, equation (15). A fractal dimension $2<D<2.36$ corresponds to an exponent between 3 and 10, and a fractal dimension $D>2.36$ to a larger exponent than 10. The k-ϕ relationship (equation 15) is of the general type of equation (3), where the factors A, B, and C in equation (15) are valid for an average type of sandstone, such as in the north German sedimentary basin. When applied to other basins, it needs to be calibrated anew.

We applied this approach to a petrophysical data set which allows a very thorough characterization of Rotliegend (Lower Permian) sandstone samples. It had been compiled over a period of 15 years in east German hydrocarbon industry laboratories. It comprises measured porosity and permeability as well as distributions of pore radii and grain sizes. With respect to this data set the average k-ϕ relationship, equation (15), tends to underestimate measured permeability, since these sandstones are characterized by a relatively large permeability at any given porosity. Therefore, the coefficients of ϕ, ϕ^2, and ϕ^{10} in the average k-ϕ relationship (equation 15) were calibrated to this data set by nonlinear regression. Minimizing the least-squares standard deviation of permeability calculated from $k = A\phi + B\phi^2 + C(10\phi)^{10}$ yields the following expression:

$$k = 155\phi + 37315\phi^2 + 630(10\phi)^{10} \quad . \qquad (16)$$

Figure 2 shows a comparison between permeability and porosity measured on different rock types and several curves calibrated to equation (3) with independent, large data sets for rocks that vary from clean and shaly sandstones to pure shales. The calibrated equation for shaly sandstone is

$$k = 6.2\phi + 1493\phi^2 + 58(10\phi)^{10} \qquad (17)$$

and for shale

$$k = 0.1\phi + 26\phi^2 + (10\phi)^{10} \quad . \qquad (18)$$

The lower four curves in Figure 2 correspond to the fractal model defined by equation (3) with exponents according to a fractal dimension D = 2.36. . They are offset due to the different effective grain radii r_{grain} which determine the coefficients of the three terms. The smallest grain radius corresponds to the lowest and most right curve for pure shales.

In contrast, the data of Bourbie and Zinszer (1985) for Fontainebleau sandstone define a curve which is quite different. This rock is characterized by strong quartz cementation. Its smooth internal surfaces correspond to a fractal dimension of D = 2. Thus it is well suited for description by the smooth grain packing model (equation 1) in which permeability varies with porosity cubed. Specifically, for porosities larger than 0.08, the permeability of Fontainebleau sandstone varies with porosity taken to a power of 3.05 (equation 2a). For smaller porosities, however, the permeability of Fontainebleau sandstone varies with porosity taken to a power of 7.33 (equation 2b). This corresponds to rougher surfaces with a fractal dimension D > 2.

2.2 Influence of chemical reactions on permeability-porosity relationship

The curves of permeability versus porosity of different rock types (see Figure 2) can be interpreted as the result of a diagenetic compaction process which starts with the initially fresh sediment. In Figure 2 the data points for permeability and porosity measured on sand by Schopper (1967) represent this starting point which is strongly influenced by the grain size distribution.

Then, during a subsequent subsidence in a sedimentary basin, porosity decreases . Generally, the major part of compaction is achieved by mechanical processes, which reduce permeability to about 10 % for temperatures below about 100 °C (Bjørkum et al., 1998). This mechanical compaction can be simulated by the fractal petrophysical model based on a constant fractal dimension. For average sandstones this leads to a power law which relates permeability to porosity taken to the tenth power. The final porosity reduction below 10 % is mainly attributed to chemical processes combined with the effects of pressure. This part of the permeability-porosity curves is characterized by a decrease of the power to which porosity is taken in the other two terms of the general permeability-porosity relationship (equation 3).

On the other hand, the smaller exponents may be due to cementation which started at an early stage of basin development, such as in the large-porosity branch of the curve for Fontainebleau sandstone. Sandstones with strong cementation are particularly interesting because the properties of reservoir sandstones depend strongly on the

amount and type of cementation. Most common is cementation by quartz due to pressure dissolution and by carbonates. Bjørkum (1996), Bjørkum and Walderhaug (1990), and Walderhaug (1996) studied and simulated these processes in detail with numerical models. The Rät sandstone in the north German sedimentary basin, which is of interest for geothermal use, provides an example for a cementation by anhydrite. Compared with average sandstones with the same effective hydraulic pore radius, cemented sandstones have a lower specific surface. They are characterized by a lower fractal dimension, which can be determined from pore radius distributions. Accordingly, the permeability-porosity relationship of cemented sandstones has a largest exponent which is smaller than 10. Permeability and porosity data measured on cores of Rät sandstone were fitted by

$$k = 0.309\,(100\phi)^{4.85} \quad (\mathrm{nm}^2) \quad . \qquad (19)$$

The data for Rät sandstone cemented by anhydrite in Figure 2 agrees well with permeability-porosity data for anhydrite rock of the Salado formation at the Waste Isolation Pilot Plant (WIPP) in New Mexico, USA (Howarth and Christian-Frear, 1997).

The permeability-porosity relationship for cemented sandstone (equation 19) was used in our simulation code's petrophysical model. It couples permeability changes to porosity changes that are induced by the precipitation and dissolution of anhydrite. As a first application, the relocation of anhydrite in a sandstone core subjected to an imposed temperature gradient during a high-pressure, high-temperature core-flooding experiment was successfully simulated.

3. CHEMICAL REACTION MODEL

A chemical reaction model was developed to calculate the amount of precipitation and dissolution of each mineral species at high temperature and salinity. It is a modification of the geochemical simulation code, PHRQPITZ (Plummer *et al.*, 1988). It permits calculations of geochemical reactions in brines and other highly concentrated electrolyte solutions using the Pitzer virial coefficient approach for the correction of activity coefficients. Reaction-modeling capabilities include calculation of aqueous speciation and mineral-saturation index as well as mineral solubility. The computed results for each aqueous solution include the osmotic coefficient, water activity, mineral saturation indices, mean activity coefficients, total activity coefficients, pH, individual-ion activities, and individual-ion activity coefficients. A data base valid for temperatures from 0 to 150 °C of Pitzer interaction parameters is provided for the system:

Na-K-Mg-Ca-H-Cl-SO_4-OH-(HCO_3-CO_3-CO_2)-H_2O.

The Pitzer treatment of the aqueous model is based largely on the equations presented by Harvie and Weare (1980), Harvie *et al*. (1984), and data of Greenberg and Moeller (1989). Data for the incorporated carbonic acid system (set in parentheses in the list above) are valid for temperatures from 0–90 °C according to He and Morse (1993). For this system and at 25 °C these data are identical to the data base of Harvie *et al*. (1984). PHRQPITZ was developed by Plummer et al. (1988) by replacing the aqueous ion-pairing model used in PHREEQE (Parkhurst *et al*., 1980) by the Pitzer virial coefficient approach (Pitzer, 1973; Pitzer and Mayorga, 1973, 1974; Pitzer and Kim, 1974; Pitzer, 1975).

We extended the PHRQPITZ code to include the calculation of temperature dependent Pitzer coefficients. At present, it still uses the Newton-Raphson approach to solve a set of algebraic equations by generating successively better estimates of the molalities and activity coefficients of the aqueous species.

In a transient coupled simulation, our chemical module first calculates any deviations from the chemical equilibrium that may exist between fluid and rock minerals. Then, for each time step of this simulation, it balances the chemical reactions necessary to reach thermodynamic equilibrium. If some reactions, for instance dissolution or precipitation of minerals, are too slow and therefore do not reach an equilibrium instantly, reaction kinetics needs to be accounted for. Therefore, and since our interest was focussed on sandstones cemented by anhydrite, the dissolution constant of anhydrite was measured in the laboratory at different temperatures and salinities.

4. NUMERICAL SIMULATION WITH COUPLED FLOW, HEAT AND SPECIES TRANSPORT, AND CHEMICALLY INDUCED PERMEABILITY CHANGES.

Our numerical code for simulating coupled flow, heat and multi-component transport, chemical reactions, and associated permeability changes is used to model the long-term behavior of a hydrothermal heat mining installation. This allows, in principle, to test different scenarios, such as:

- A potential self-sealing of the exploited reservoir by precipitation of minerals with prograde solubility around the injection well;
- The redistribution of minerals with retrograde solubility by precipitation at the warm temperature front. This partial and transient sealing may either diminish or increase the efficiency of heat mining in the reservoir. On the one hand a slight reduction in permeability which moves through the reservoir with the warm temperature front may diverge the direct flow between the injection and the production well and thus increase the reservoir volume which is cooled. On the other hand, if the sealing is too strong, the overall flow rate may drop so much that the efficiency is damaged;
- Possible technical measures to prevent the undesired effects;
- The influence of the position of the boreholes in the reservoir and in respect to each other, pumping rates, injection temperature, and other factors on these processes.

This way, the long-term performance of such an installation as well as the safety of the investment can be better estimated.

CONCLUSIONS

A new numerical tool was developed for simulating the operation of a hydrothermal heat mining installation over a period of 30-50 years. Different production/injection regimes and different types of fluid mineralization can be accommodated. Critical scenarios focus around the

injection well where chemical equilibrium is perturbed due to lower temperatures or changes in pH value compared to the reservoir. At the propagating temperature front all processes involved interact with each other in a complex way. Chemical reactions causing dissolution and precipitation of minerals induce porosity and permeability changes. The permeability-porosity relationship is not trivial and depends on the particular structure of the precipitating mineral surface which is expressed by a specific fractal dimension.

Based on a fractal model for porous rocks, new relations were established in which effective radius, tortuosity and porosity are connected through the fractal dimension D. A default value of $D = 2.36$ was shown to be useful for the interpretation of data from an ensemble of Rotliegend (Lower Permian) sandstone samples. Permeability can be estimated from a power-law relation between permeability and porosity. This fractal model is flexible and applicable over a wide range of porosities, and it can be adjusted to different rock types. The average fractal permeability-porosity relationship was successfully calibrated to a comprehensive data set measured on Rotliegend sandstone samples. A group of variants of this correspond to different types of sandstones ranging from clean to shaly. When applying this relationship to a specific basin, however, its coefficients need to be determined anew, based on core data from this specific basin. Different types of permeability-porosity curves are discussed in relation to different processes of diagenesis such as mechanical compaction, cementation and pressure dissolution.

In conclusion, the new approach based on a fractal pore-space geometry provides a simple and versatile technique to estimate permeability changes due to porosity changes caused by mineral reactions during the operation of geothermal installations. The simulation tool permits to evaluate different scenarios in respect to the long-term performance of a hydrothermal heat mining installation and should be helpful to assess the security of such a major investment.

ACKNOWLEDGMENTS

The research reported in this paper was supported by the German Federal Ministry for Education, Science, Research, and Technology (BMBF) under grant 032 69 95.

REFERENCES

Bjørkum. P.A. (1996). How important is pressure in causing dissolution of Quartz in sandstones? *J. Sedimentary Res.*, Vol. 66 (1), pp. 147-154.

Bjørkum, P.A. and Walderhaug, O. (1990). Geometrical arrangement of calcite cementation within shallow marine sandstones. *Earth-Science Rev.*, Vol. 29, pp. 145-161.

Bjørkum. P.A., Oelkers, E.H., Nadeau, P.H., Walderhaug, O., and Murphy, W.M. (1998). Porosity prediction in quartzose sandstone as a function of time, temperature, depth, stylolite frequency, and hydrocarbon saturation. *AAPG Bulletin*, Vol. 82 (4), pp. 637-648.

Bourbie, T. and Zinszner, B. (1985). Hydraulic and acoustic properties as a function of porosity in Fontainebleau sandstone. *J. Geophys. Res*., Vol. 90 (B13), pp. 11524-11532.

Carman, P. C. (1956). *Flow of gases through porous media*. Butterworth Scientific Publications, London.

David, C., Wong, T., Zhu, W., and Zhang, J. (1994). Laboratory measurements of compaction-induced permeability change in porous rocks: implications for the generation and maintenance of pore pressure excess in the crust. *Pure Appl. Geophys*, Vol. 143 (1/2/3), pp. 425-456.

Greenberg J.P. & Moeller N. (1989). The prediction of mineral solubilities in natural waters: A chemical equilibrium model for the Na-K-Ca-Cl-SO4-H2O system to high concentration from 0 to 250 °C, *Geochim. Cosmochim. Acta*, Vol. 53, pp. 2503-2518.

Harvie, C.E., Moeller, N., and Weare, J.H. (1984). The prediction of mineral solubilities in natural waters: The Na-K-Mg-Ca-H-Cl-SO4-OH-HCO3-CO3-CO2-H2O system to high ionic strengths at 25°C. *Geochim. Cosmochim. Acta*, Vol. 48, pp. 723-751.

Harvie, C.E. and Weare, J.H. (1980). The prediction of mineral solubilities in natural waters: the Na-K-Mg-Ca-Cl-SO4-H2O system from zero to high concentration at 25 °C. *Geochim. Cosmochim. Acta*, Vol. 44, pp. 981-997.

He, S. and Morse, J.W. (1993). The carbonic acid system and calcite solubility in aqueous Na-K-Ca-Mg-Cl-SO4 solutions from 0-90°C. *Geochim. Cosmochim. Acta*, Vol. 57, pp. 3533-3554.

Howarth, S.M. and Christian-Frear, T. (1997). Porosity, Single-Phase Permeability, and capillary pressure data from preliminary laboratory experiments on selected samples from marker bed 139 at the Waste Isolation Pilot Plant. *Sandia report*, SAND94-0472/1, Vol. 1.

Pape, H., Clauser, C. and Iffland, J. (1999). Permeability prediction based on fractal pore-space geometry. *Geophysics*, Vol. 64(6), pp. 1447-1460.

Pape, H., Riepe, L., and Schopper, J. R. (1982). A pigeon-hole model for relating permeability to specific surface. *The Log Analyst,* Vol. 23 (1), pp. 5-13; Errata. *The Log Analyst*, Vol. 23 (2), p. 50.

Pape, H., Riepe, L., and Schopper, J. R. (1984). The role of fractal quantities, as specific surface and tortuosities, for physical properties of porous media. *Particle Characterization*, Vol. 1, pp. 66-73.

Pape, H., Riepe, L., and Schopper, J. R. (1987a). Theory of self-similar network structures in sedimentary and igneous rocks and their investigation with microscopical methods. *J. Microscopy*, Vol. 148, pp. 121-147.

Pape, H., Riepe, L., and Schopper, J. R. (1987b). Interlayer conductivity of rocks - a fractal model of interface irregularities for calculating interlayer conductivity of natural porous mineral systems. *Colloids and Surfaces*, Vol. 27, pp. 97-122.

Pape H., and Schopper, J.R., (1988).Relations between physically relevant geometrical properties of a multi-fractal porous system, *Studies in Surface Science and Catalysis,* Vol. 39, pp 473-482.

Parkhurst, D.L., Thorstenson, D.C., and Plummer, L.N. (1980). PHREEQE--a computer program for geochemical calculations: U.S. *Geological Survey Water-Resources Investigations Report,* Vol. 80-96, pp. 1-195. (Revised and reprinted, 1990.)Pitzer, K.S. (1973). Thermodynamics of electrolytes. 1. Theoretical basis and general equations: *J. Physical Chemistry*, Vol. 77, pp. 268-277.

Pitzer, K.S. (1975). Thermodynamics of electrolytes. 5. Effects of higher-order electrostatic terms. *J. Solution Chemistry*, Vol. 4, pp. 249-265.

Pitzer, K.S. and Kim, J.J. (1974). Thermodynamics of electrolytes. 4. Activity and osmotic coefficients for mixed electrolytes. *J. Amer. Chem. Soc.*, Vol. 96, pp. 5701-5707.

Pitzer, K.S. and Mayorga, G., 1973, Thermodynamics of electrolytes. 2. Activity and osmotic coefficients for strong electrolytes with one or both ions univalent. *J. Physical Chemistry*, Vol. 77, pp. 2300-2308.

Pitzer, K.S. and Mayorga, G. (1974). Thermodynamics of electrolytes. 3. Activity and osmotic coefficients of 2-2 electrolytes. *J. Solution Chemistry*, Vol. 3, p. 539-546.

Plummer, L.N., Parkhurst, D.L., Fleming, G.W., and Dunkle, S.A. (1988). A computer program incorporating Pitzer's equations for calculation of geochemical reactions in brines. *U.S. Geological Survey Water-Resources Investigations Report*, Vol. 88-4153, pp. 1-310.

Schopper, J. R. (1967). Experimentelle Methoden und eine Apparatur zur Untersuchung der Beziehungen zwischen hydraulischen und elektrischen Eigenschaften loser und künstlich verfestigter poröser Medien. *Geophysical Prospecting*, Vol.15 (4), pp. 651-701.

Shashwati, R. and Tarafdar, S. (1997). Archie's law from a fractal model for porous rocks. *Physical Review B*, Vol. 55(13), pp. 8038-8041.

Ungerer, P., Burrus, J., Doligez, B., Chénet, P. Y., and Bessis, F. (1990). Basin evaluation by integrated two-dimensional modeling of heat transfer, fluid flow, hydrocarbon generation, and migration. *AAPG Bull.,* Vol. 74 (3), pp. 309-335.

Van der Marck, S. (1999). Evidence for a nonzero transport threshold in porous media. *Water Resour. Res*., Vol. 35 (2), pp. 595-599.

Walderhaug, O. (1996). Kinetic modeling of quartz cementation and porosity loss in deeply buried sandstone reservoirs. *AAPG Bulletin*, Vol. 80 (5), pp.731-745.

Zhu, W., David, C., and Wong, T. (1995). Network modeling of permeability evolution during cementation and hot isostatic pressing. *J. Geophys. Res*., Vol. 100 (B8), pp. 15451-15464.

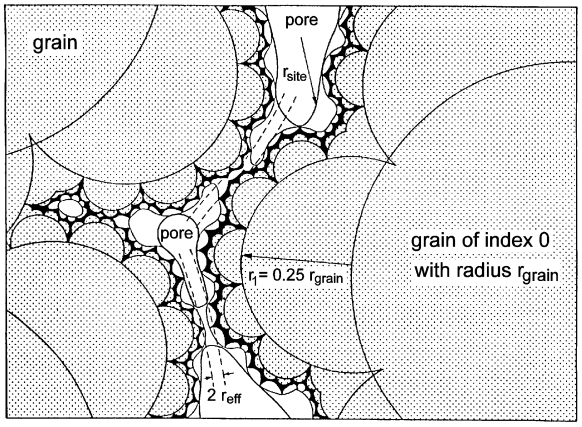

Figure 1: Cartoon of a sedimentary rock according to the fractal "pigeon hole" model showing geometrical pores with radii r_{site} and hydraulic model capillaries with effective radii r_{eff}

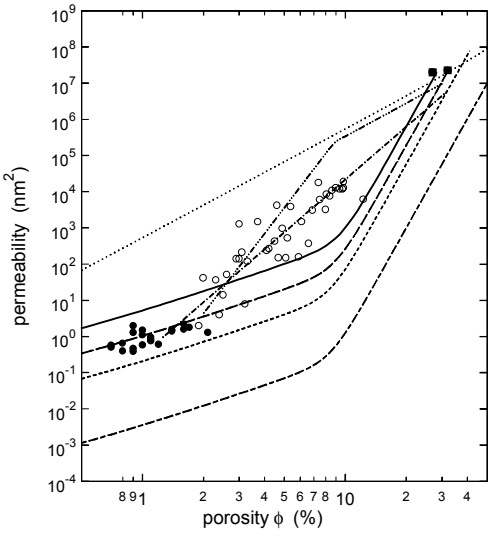

Figure 2: Permeability versus porosity for different consolidated and unconsolidated clean and shaly sandstones (Symbols: measured permeability and porosity; lines : fractal k-ϕ relationships)